To link to this article : DOI: 10.1016/S1466-6049(00)00047-7
http://dx.doi.org/10.1016/S1466-6049(00)00047-7

X-ray photoelectron spectroscopic study of non-stoichiometric nickel and nickel–copper spinel manganites

C. Drouet[a], C. Laberty[a], J.L.G. Fierro[b], P. Alphonse[a,*], A. Rousset[a]

[a] *Laboratoire de Chimie des Matériaux Inorganiques et Energétiques, Université Paul Sabatier, 118 Route de Narbonne, 31062 Toulouse Cedex 04, France*

[b] *Instituto de Catálisis y Petroleoquímica, Cantoblanco, 28049 Madrid, Spain*

Abstract

The surface of non-stoichiometric nickel and nickel–copper spinel manganites has been investigated by X-ray Photoelectron Spectroscopy (XPS). The oxidation states of the nickel, copper and manganese cations present on the surface of the samples were determined from the analysis of the M $2p_{3/2}$ core levels (M=Ni, Cu, Mn). In particular, both Cu^{2+} and Cu^{+} were evidenced in the structure whereas only bivalent nickel was observed. The partial substitution of manganese by copper led to a chemical shift towards lower binding energy in the Ni $2p_{3/2}$ region, which was explained by the displacement of some Ni^{2+} cations from tetrahedral to octahedral sites of the spinel structure. Finally, the surface atomic ratios Ni/Mn for nickel manganites, Ni/(Mn+Cu) and Cu/(Mn+Ni) for nickel–copper manganites, determined from XPS data, were compared to the ratios corresponding to the bulk composition. This study shows in all cases a nickel enrichment at the surface which is not affected by the copper content of the oxide. On the contrary, the ratio Cu/(Mn+Ni) was found to be lower than the corresponding bulk value.

Keywords: A. oxides; A. surfaces; C. photoelectron spectroscopy; D. electronic structure

1. Introduction

Many studies have been conducted on the surface chemistry and characterization of nickel and nickel–copper manganites. However, a controversy remains concerning the oxidation states of the cations and their distribution among the tetrahedral and octahedral sites of the spinel structure. A typical example of discordance concerns the presence of Ni^{3+} cations in these samples [1–3].

Recent catalytic experiments [4] have shown the important activity of these non-stoichiometric oxides towards CO oxidation and NO reduction. Hence, the knowledge of the oxidation states of the cations present in these oxides, and particularly on their surface, is of great interest for the understanding of such reactions.

The present study aims at determining the oxidation states of the nickel, copper and manganese cations present on the surface of non-stoichiometric nickel and nickel–copper manganites. The technique used was the X-ray Photoelectron Spectroscopy (XPS) which provides powerful and direct analysis of the surface. From the XPS results, surface atomic ratios were determined and compared to bulk ratios to study possible surface deviations from stoichiometry.

*Corresponding author. Tel.: +33-561-556-285; fax: +33-561-556-163.

2. Experimental

2.1. Preparation of the samples

Non-stoichiometric nickel and nickel–copper spinel manganites, corresponding to the general formula $Ni_xCu_yMn_{3-x-y}\square_{3\delta/4}O_{4+\delta}$ (where $y=0$ for nickel manganites, and $\square$ stands for the cation vacancies) were synthesized by thermal decomposition of mixed oxalates $Ni_{x/3}Cu_{y/3}Mn_{(3-x-y)/3}C_2O_4,nH_2O$ at 623 K in air for 6 h (heating rate: 2 K/min, cooling rate: 5 K/min). These oxalate precursors were precipitated at room temperature by quick introduction of an aqueous solution of nickel, copper and manganese nitrates (0.2 M nitrates) into an aqueous solution of ammonium oxalate 0.2 M at room

temperature under stirring. After 30 min, the precipitate was filtered, washed with deionized water and dried at 360 K in air. X-ray diffraction only showed pure cubic spinel phases [5]. The nominal composition of the oxides was determined by ionic chromatography (Dionex DX100, cationic column CS5). The detailed characterization of these oxides is available elsewhere [5].

2.2. XPS experiments

X-ray photoelectron spectra were acquired with a VG ESCALAB 200R spectrometer equipped with a hemispherical electron analyzer and Mg Kα ($h\nu = 1253.6$ eV, 1 eV $= 1.6302 \times 10^{-19}$ J) 120 W X-ray source. The powder samples were heated in the pretreatment chamber of the instrument at 573 K under 500 Torr O_2 (1 Torr = 133.3 Pa) for 1 h. The residual pressure in the ion-pumped analysis chamber was maintained below 5×10^{-9} Torr during data acquisition. The intensity of each peak was estimated from integration after having smoothed, subtracted an 'S-shaped' background and fitted the experimental curve to a combination of Gaussian-Lorentzian lines. The binding energies (BE) were referenced to the C 1s peak (atmospheric contamination) at 284.6 eV. This reference gives BE values with an accuracy of ±0.1 eV.

3. Results and discussion

Non-stoichiometric nickel and nickel–copper spinel manganites are highly divided materials that exhibit large specific areas (Sw > 100 m^2/g). These oxides present a non-stoichiometric level δ ranging from 0.2 to 0.7 that depends on the nickel and copper contents as well as on the decomposition temperature of the oxalate precursor [5]. The characteristics (Sw and δ) of the samples studied in this work are reported in Table 1. The non-stoichiometry of these compounds is due to the presence in the spinel structure of cations with higher oxidation states than in stoichiometric counterparts. The presence of cation vacancies allows to preserve the overall electrical neutrality of the crystals. Drouet et al. [5] showed using thermal analyses that the heating of such oxides in argon up to 873 K leads to the corresponding stoichiometric oxides by oxygen release, which enables the measure of δ. The resulting reduction profiles present several steps, associated very likely to the reduction of specific cations within the structure. In order to determine the oxidation states of the metals involved here, the M 2p regions (where M stands for Ni, Mn or Cu) were analyzed by X-ray photoelectron spectroscopy (XPS).

Table 1
Specific surface area (Sw) and non-stoichiometry (δ) of the oxides $Ni_xCu_yMn_{3-x-y}\square_{3\delta/4}O_{4+\delta}$

Oxide composition		Sw (m^2/g)	δ
x_{Ni}	y_{Cu}		
0.45	0	165	0.43
0.70	0	180	0.70
0.84	0	250	0.60
1.05	0	250	0.43
0.70	0.65	160	0.27
0.70	0.75	155	0.25
0.70	0.91	140	0.22

Fig. 1 shows the Ni 2p core-level spectra for the nickel manganite samples $Ni_xMn_{3-x}\square_{3\delta/4}O_{4+\delta}$ with $x_{Ni} = 0.45$, 0.70, 0.84 and 1.05. For the sake of clarity, only the Ni $2p_{3/2}$ region is presented as deconvoluted into all its components. For all these samples, three peaks (referred as I, II and III in Fig. 1) could be found in the range from 845 to 865 eV and their characteristics are given in Table 2. Peak I, which appears at a binding energy (BE) of 852–853 eV, can be attributed to Ni^{2+} cations within the spinel structure. Indeed, this BE value matches those given in the literature for nickel-containing compounds [2,6]. Moreover peak III, which lies at ca. 7 eV above peak I, is assigned to the well known shake-up satellite line of Ni^{2+}. On the contrary, peak II appears at too high BE (ca. 857 eV) to be assignable to Ni^{2+} cations in octahedral or tetrahedral sites

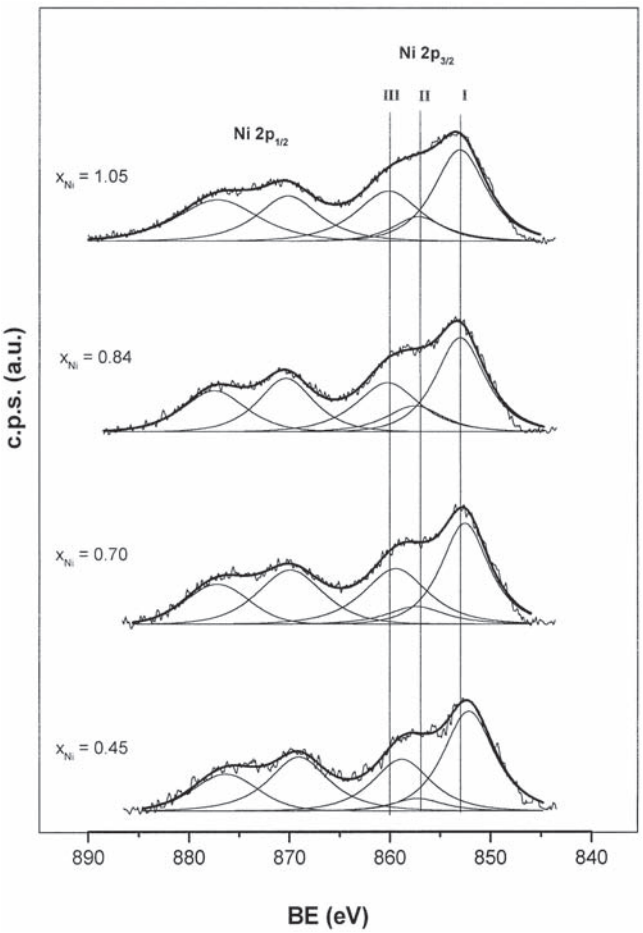

Fig. 1. Ni 2p core-level spectra for $Ni_xMn_{3-x}\square_{3\delta/4}O_{4+\delta}$ with $x_{Ni} = 0.45$, 0.70, 0.84 and 1.05.

Table 2
XPS characteristics of peaks I, II and III from the Ni $2p_{3/2}$ region of nickel manganites Ni $2p_{3/2}$ region of nickel manganites

Ni $2p_{3/2}$ region			
x_{Ni} in $Ni_xMn_{3-x}\square_{3\delta/4}O_{4+\delta}$	Binding energy (eV)		
	Peak I	Peak II	Peak III
1.05	853.1 (6.0)[a]	857.3(5.9)	860.2(7.6)
0.84	852.9 (5.8)	857.5(6.6)	860.1(7.3)
0.70	852.5 (5.6)	857.3(6.7)	859.5(7.4)
0.45	852.2 (5.8)	857.2(6.5)	858.9(7.5)

[a] Numbers in parentheses refer to the FWHM in eV.

of the spinel structure. This binding energy could rather correspond to Ni^{3+} cations or surface nickel hydroxide species [2,3,6]. In order to shed some light on this point, the O 1s region was also investigated. The shape analysis of the corresponding spectra showed the presence of two peaks at 529–530 eV (main component) and ca. 531 eV (minor component). The example of the oxide $Ni_{0.70}Mn_{2.30}\square_{0.53}O_{4.70}$ is reported in Fig. 2. It is obvious from literature results that the main peak at 529.7 eV is related to the oxygen anions O^{2-} bound to the metal cations of the structure, while the minor component at 531 eV can be attributed to surface metal hydroxyl groups [6]. The presence of such hydroxide species has already been observed by several authors in the case of oxide samples [2,7,8]. These findings tend thus to show that peak II of the Ni $2p_{3/2}$ region can certainly be assigned to nickel hydroxide rather than Ni^{3+} cations. Moreover, such trivalent nickel ions are relatively unstable species and would have certainly been reduced to Ni^{2+} under ultrahigh vacuum.

From the XP spectra of nickel–copper manganites, the same conclusions could be drawn concerning the occurrence of three peaks in the Ni $2p_{3/2}$ region. However, as a general trend, the binding energies of these peaks are shifted towards lower values when compared to those of nickel manganites. Table 3 shows the characteristics of peaks I, II and III for oxides with constant nickel composition $x_{Ni}=0.70$ and different copper contents. A chemical shift of peaks I and III of ca. -1.5 eV can be observed

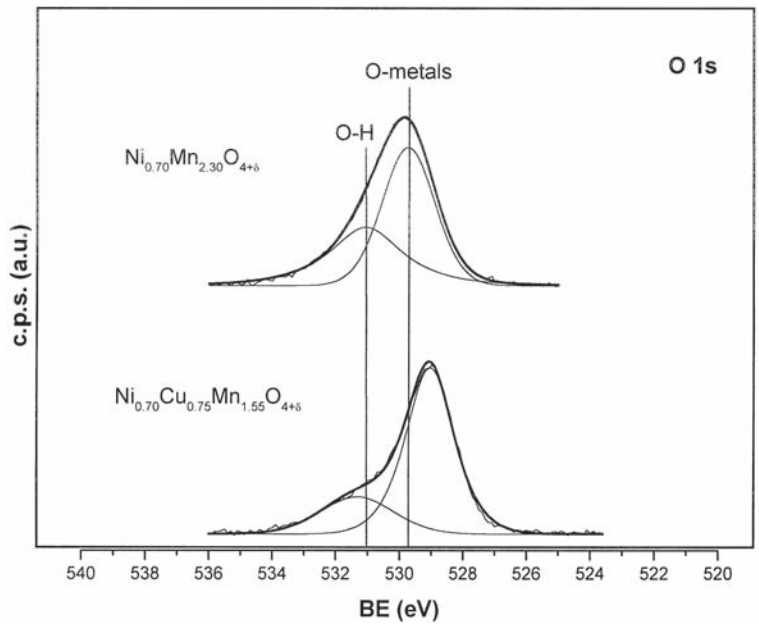

Fig. 2. O ls core-level spectra of the O ls region for $Ni_{0.70}Mn_{2.30}\square_{0.53}O_{4.70}$ and $Ni_{0.70}Cu_{0.75}Mn_{1.55}\square_{0.19}O_{4.25}$.

Table 3
XPS characteristics of peaks I, II and III from the Ni $2p_{3/2}$ region of nickel–copper manganites with $x_{Ni}=0.70$

Ni $2p_{3/2}$ region			
y_{Cu} in $Ni_{0.70}Cu_yMn_{2.3-y}\square_{3\delta/4}O_{4+\delta}$	Binding energy (eV)		
	Peak I	Peak II	Peak III
0	852.5 (5.6)[a]	857.3 (6.7)	859.5 (7.4)
0.65	851.2 (6.2)	856.7 (7.2)	858.1 (7.5)
0.75	851.1 (6.6)	857.0 (6.1)	858.1 (6.9)
0.91	851.1 (6.7)	857.1 (7.3)	858.0 (7.0)

[a] Numbers in parentheses refer to the FWHM in eV.

for copper-containing compounds compared to nickel manganites.

Several authors have already reported such chemical shifts. Different causes may be at the origin of a decrease in binding energy and the most currently invoked is a reduction of the element. However, the Ni^{2+} cations could not be reduced under the experimental conditions used in this study. Moreover, the presence of the satellite line (peak III) with similar intensities in all cases indicates that bivalent nickel is still present in the structure. A second possible explanation for this shift could be the weakening of the Ni–O bonds when copper is incorporated into the structure. Indeed, the analysis of the O 1s region corresponding to a nickel and a nickel–copper manganite with the same nickel content (Fig. 2) shows that there is a slight decrease in BE of the corresponding oxygen peak when copper is present in the structure. However, the small shift observed in the O 1s region cannot explain totally the decrease of ca. −1.5 eV in BE for the Ni $2p_{3/2}$ core level of copper-containing samples. A third possible cause for such chemical shifts could be the change of coordination, octahedral (Oh) or tetrahedral (Td), of the Ni^{2+} cations within the spinel structure. Indeed, several authors have shown that the binding energy obtained for a cation in octahedral sites is generally smaller than in tetrahedral sites [9,10].

Navrostsky and Kleppa [11] have calculated from thermodynamic measurements the site preference energy of several bivalent and trivalent cations within the spinel structure. This study showed in particular the octahedral preference of Mn^{3+}, Ni^{2+} and Cu^{2+} in the order $Mn^{3+} > Ni^{2+} > Cu^{2+}$. It is worthwhile noting that tetravalent manganese cations Mn^{4+} have also a marked preference for octahedral sites. On the contrary, Mn^{2+} and Cu^{+} present a high tendency for occupying tetrahedral sites. However, in some cases, these energetic considerations have been partly thwarted by experimental results. A typical example is that of nickel manganite $NiMn_2O_4$ which was shown to exhibit a good electrical conductivity whereas its theoretical cation distribution $Mn^{2+}[Ni^{2+}Mn^{4+}]O_4^{2-}$ would have led to an insulator. In this case, the measured conductivity can only be explained by the presence of part of the Ni^{2+} cations in tetrahedral sites. This implies the following cationic distribution: $Ni_{\lambda}^{2+}Mn_{1-\lambda}^{2+}[Ni_{1-\lambda}^{2+}\ Mn_{2\lambda}^{3+}\ Mn_{1-\lambda}^{4+}]O_4^{2-}$ which can explain the hopping of electrons between Mn^{3+} and Mn^{4+} cations located in octahedral sites. The presence of Ni^{2+} cations in tetrahedral sites is now well-adopted in nickel manganites with high nickel contents [3,12,13]. Another controversial point concerns the presence of Cu^{2+} cations exclusively in octahedral sites. Several studies [13–17] have indeed pointed out the presence of part of the bivalent copper in a tetrahedral environment. In the case of copper-containing spinels, most authors agree with the presence of monovalent copper in tetrahedral sites and bivalent copper in both octahedral and tetrahedral sites [13,14,18]. The incorporation of copper into the nickel manganite structure leads thus to an increasing amount of cations in tetrahedral sublattices, which induces the displacement of some Ni^{2+} cations from tetrahedral to octahedral sites. Such a change can indeed explain the chemical shift of ca. −1.5 eV observed in the Ni $2p_{3/2}$ region between nickel and nickel–copper manganites. These results remind those of Allen et al. [9] in the case of nickel–iron chromites.

The analysis of the Cu $2p_{3/2}$ region for the nickel–copper manganites shows the presence of four peaks in the range from 925 to 945 eV. Fig. 3 displays the Cu $2p_{3/2}$ core-level spectra for $Ni_{0.70}Cu_yMn_{2.3-y}\square_{3\delta/4}O_{4+\delta}$ with $y_{Cu} = 0.65$, 0.75, 0.91. The characteristics of these peaks are reported in Table 4. The binding energy found in the literature for the main Cu $2p_{3/2}$ peak of the oxide CuO is close to 933.6 eV, whereas its well known shake-up satellite line generally lies between 940 and 945 eV. However, various studies [14,16,17] showed that the position of these peaks depends on the chemical composition of the sample and particularly on the near environment of the copper cations. For example, Brabers and Van Setten [19] reported a BE of 932.6 eV for Cu^{2+} cations in $CuMnCoO_4$, that is 1 eV below the value found

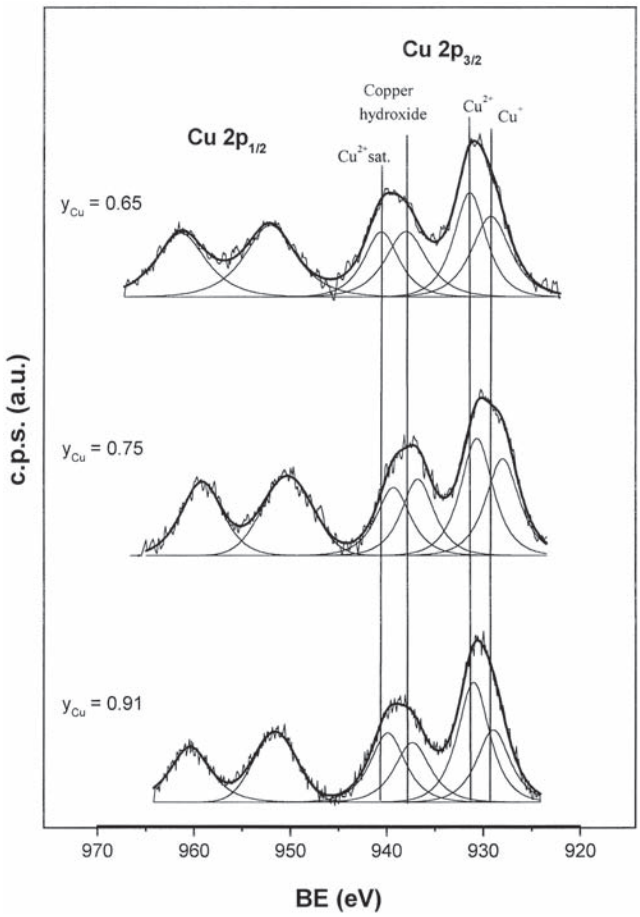

Fig. 3. Cu 2p core-level spectra for $Ni_{0.70}Cu_yMn_{2\cdot3-y}\square_{3\delta/4}O_{4+\delta}$ with $y_{Cu} = 0.65$, 0.75 and 0.91.

Table 4
XPS data of the Cu $2p_{3/2}$ region of nickel–copper manganites with $x_{Ni}=0.70$

Cu $2p_{3/2}$ region						
y_{Cu} in $Ni_{0.70}Cu_yMn_{2.3-y}\square_{3\delta/4}O_{4+\delta}$	Binding energy (eV)					
	Cu^+	Cu^{2+}	Cu hydroxide	Cu^{2+} sat.	I(Cu^+)[b]	I(Cu^{2+})[c]
0.65	929.3 (4.7)[a]	931.4 (3.9)	938.0 (4.9)	940.6 (4.2)	28%	50%
0.75	928.1 (4.1)	930.7 (3.9)	936.8 (4.0)	939.3 (4.1)	27%	52%
0.91	929.0 (4.0)	931.0 (3.8)	937.4 (4.3)	939.9 (4.2)	22%	58%

[a] Numbers in parentheses refer to the FWHM in eV.
[b] Intensity of the Cu^+ peak in% of the total Cu $2p_{3/2}$ area.
[c] Total intensity of the Cu^{2+} peaks (main peak and sat.) in% of the total Cu $2p_{3/2}$ area.

for CuO. In our case, the main peak of the Cu $2p_{3/2}$ region is located at ca. 931 eV, which is close to Brabers and Van Setten's results. Therefore, this peak can be attributed to bivalent copper ions within the spinel structure. Moreover, the peak observed at ca. 940 eV corresponds to the position of the satellite line of Cu^{2+} found in the literature [6,19] and remains closely linked to the position of the main peak (at 8–9 eV above the main peak). The high intensity of this satellite peak is an additional element in favor with the assignment of the main peak (at ca. 931 eV) to Cu^{2+}.

Previous studies [14–17] have shown that it was possible in some cases to distinguish between octahedrally and tetrahedrally coordinated cations. Although the presence of Cu^+ cations in octahedral sites is still a matter of controversy, most authors agree that the order of binding energies in the Cu $2p_{3/2}$ region is as follows: $Cu^+(Oh)<Cu^+(Td)<Cu^{2+}(Oh)<Cu^{2+}(Td)$. However, in the present case, such a distinction between octahedrally and tetrahedrally coordinated Cu^{2+} cations was not possible. Therefore, the main peak at ca. 931 eV may include Cu^{2+} located in both Oh and Td sites. Brabers and Van Setten [19] have attributed a peak at 930.5 eV in the Cu $2p_{3/2}$ region to tetrahedrally coordinated Cu^+ cations in $CuMnCoO_4$. This value is close to that of the peak observed at 928–929.5 eV in this study. However, metallic copper Cu^0 corresponds to similar BE values as Cu^+ [6] and it is generally not possible to distinguish between these oxidation states only from XPS analysis of the Cu 2p region. To achieve this goal, the Cu $L_3M_{45}M_{45}$ Auger electron transition was recorded (Fig. 4) and the modified Auger parameter α' was determined by the formula $\alpha'=h\nu+(\text{KE Cu}_{LMM}-\text{KE Cu }2p_{3/2})$, where $h\nu$ is the energy of the incident photon, and KE Cu_{LMM} and KE $Cu2p_{3/2}$ are the kinetic energies corresponding to the Cu $L_3M_{45}M_{45}$ and Cu $2p_{3/2}$ core-levels, respectively. The modified Auger parameter found for all the oxides was $\alpha'\cong 1846.6$–1848.1 eV. On the other hand, the parameter corresponding to Cu^0 is generally considered to be close to 1851 eV whereas that of Cu^+ is much smaller: 1848–1849 eV [6,20]. This last value matches our experimental results. Therefore, the peak at 928–929.5 eV can be attributed to Cu^+ cations and not to metallic copper atoms. These results are in agreement with several studies [2,16,18] that point out the presence of both monovalent and bivalent copper in the Ni–Cu–Mn–O system.

The peak at ca. 936.5–938 eV in the Cu $2p_{3/2}$ region is more difficult to attribute. Indeed, there are no data reported in the literature that fits these results for copper cations within the spinel structure. Hence, this peak is related to a different coordination environment of the copper. The XPS peak analysis of the Ni 2p and O 1s core

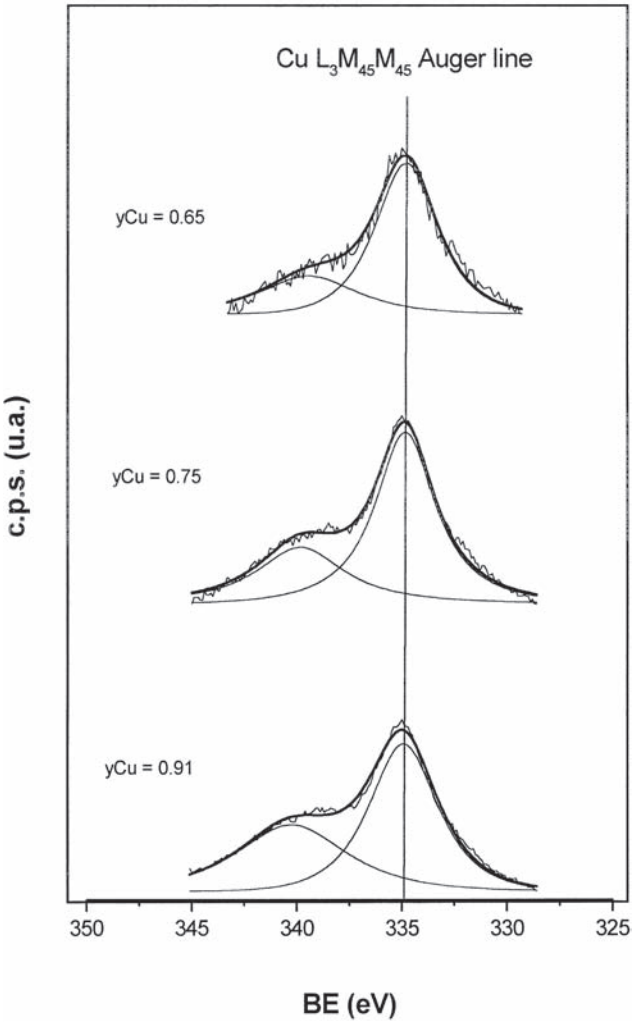

Fig. 4. Cu $L_3M_{45}M_{45}$ Auger transition for $Ni_{0.70}Cu_yMn_{2.3-y}\square_{3\delta/4}O_{4+\delta}$ with $y_{Cu}=0.65$, 0.75 and 0.91.

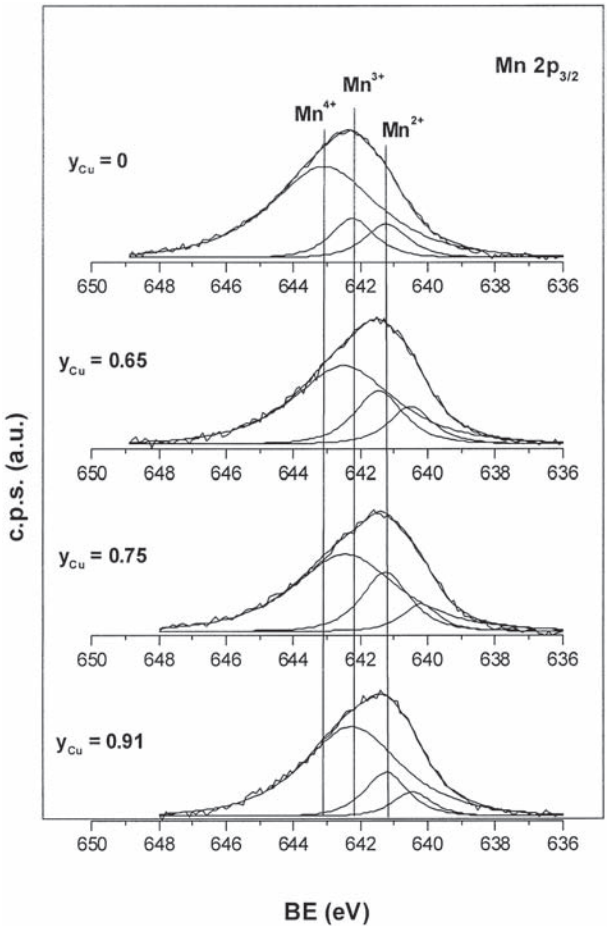

Fig. 5. Mn2$p_{3/2}$ core-level spectra for $Ni_{0.70}Cu_yMn_{2.3-y}\square_{3\delta/4}O_{4+\delta}$ with $y_{Cu}=0$, 0.65, 0.75 and 0.91.

levels showed the presence of hydroxide species on the surface of such oxides. Hence, the peak observed at 936.5–938 eV in the Cu $2p_{3/2}$ region of these oxides may be related to surface copper hydroxide.

Table 4 shows that the relative intensity of the peak located at 928–929.5 eV in the Cu $2p_{3/2}$ region, attributed to monovalent copper, tends to decrease when the nominal copper content of the oxide increases. On the contrary, the total intensity of the peaks relative to Cu^{2+} cations in the spinel structure, i.e. taking into account the main peak as well as its satellite line, displays the opposite behavior. The increase in copper content of the oxides favors thus bivalent copper rather than monovalent Cu^{+} cations.

Many papers have reported XPS data of manganese-containing compounds. These studies have shown that it was generally possible to distinguish between the different oxidation states of manganese from the analysis of the Mn 2p or Mn 3p regions [1,3,21,22]. In particular, Hashemi and Brinkman [1] have attributed a peak at 640.3 eV in the Mn $2p_{3/2}$ region to Mn^{2+} cations in $NiMn_2O_4$, whereas peaks at 641.2 eV and 642.0 eV were assigned respectively to Mn^{3+} and Mn^{4+}. In our study, the Mn $2p_{3/2}$ region for nickel and nickel–copper manganites could be deconvoluted into three peaks at 640.2–641.6 eV, 641.2–642.6 eV and 642.3–643.8 eV (Fig. 5). The characteristics of these peaks for all the compounds studied in this work are listed in Table 5. According to the literature data, the three peaks were attributed respectively to Mn^{2+}, Mn^{3+} and Mn^{4+} cations within the spinel structure (satellite lines of manganese appear at much higher binding energies [1,14]). These assignments are consistent with the cation distributions found in the literature showing the coexistence of the three oxidation states of the manganese [1,3,21,22]. A slight decrease in binding energy can be observed in the Mn $2p_{3/2}$ region (Fig. 5) for Ni–Cu compounds compared to nickel manganites. This small shift is close to that observed in the O 1s region and might be assigned to a slight weakening of the Mn–O bonds in the presence of copper.

Table 5 also reports the proportions of the three oxidation states of the manganese as determined from the Mn $2p_{3/2}$ core level analysis. Except for the oxide $Ni_{0.45}Mn_{2.55}\square_{0.32}O_{4.43}$, the percentages of Mn^{2+} and Mn^{3+} in the spinel structure are in the range 8–24%, while that of Mn^{4+} is close to 70%. Such proportions of tetravalent manganese match those expected in the case of non-stoichiometric compounds. This shows that the samples have not been notably reduced during the XPS experiments. The particular behavior of the oxide $Ni_{0.45}Mn_{2.55}\square_{0.32}O_{4.43}$ can be explained by the absence of

Table 5
XPS data of the Mn $2p_{3/2}$ region for nickel and nickel–copper manganites (with $x_{Ni}=0.70$)

Mn $2p_{3/2}$ region							
Oxide composition		Binding Energy (eV)			Peak Intensity[b] (%)		
x_{Ni}	y_{Cu}	Mn^{2+}	Mn^{3+}	Mn^{4+}	$I(Mn^{2+})$	$I(Mn^{3+})$	$I(Mn^{4+})$
0.45	0	641.0 (2.5)[a]	642.1 (2.3)	643.0 (3.9)	42	23	35
0.70	0	641.4 (2.0)	642.5 (1.8)	643.5 (3.7)	11	13	76
0.84	0	641.6 (2.0)	642.6 (1.9)	643.5 (3.7)	16	18	66
1.05	0	641.1 (2.0)	642.2 (1.9)	643.8 (3.7)	17	16	67
0.70	0.65	640.5 (1.5)	641.5 (1.7)	642.5 (3.5)	13	22	65
0.70	0.75	640.2 (1.3)	641.3 (1.7)	642.5 (3.6)	8	24	68
0.70	0.91	640.4 (1.3)	641.2 (1.5)	642.3 (3.4)	8	16	76

[a] Numbers in parentheses refer to the FWHM in eV.
[b] Intensity of the peak in % of the total Mn $2p_{3/2}$ area.

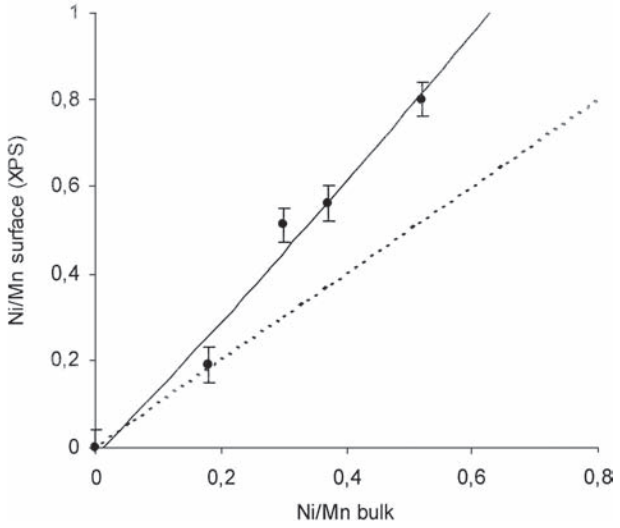

Fig. 6. Comparison of the surface (XPS) and bulk Ni/Mn atomic ratios for nickel manganites.

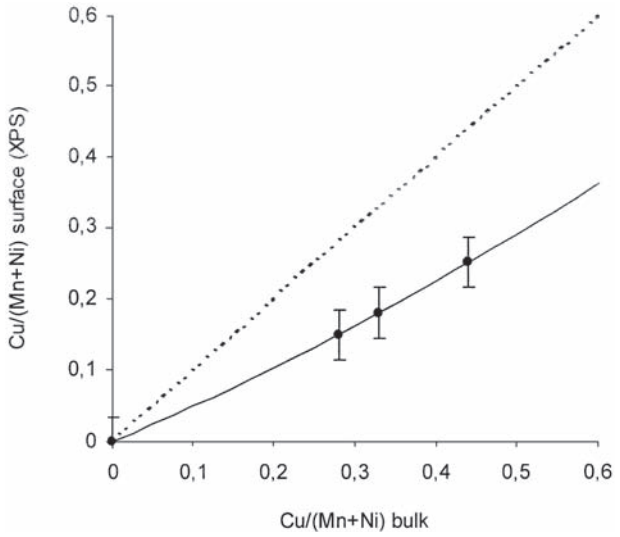

Fig. 7. Comparison of the surface (XPS) and bulk CuI(Mn + Ni) atomic ratios for nickel–copper manganites.

nickel cations in tetrahedral sites (unlike the other oxides with higher nickel contents), which enables a higher amount of Mn^{2+} in Td sites as can be seen in Table 5. Finally, the comparison of $Ni_{0.70}Mn_{2.3}\square_{0.53}O_{4.70}$ and $Ni_{0.70}Cu_yMn_{2.3-y}\square_{3\delta/4}O_{4+\delta}$ with $y_{Cu} = 0.65$, 0.75, 0.91 (Table 5) shows similar proportions respectively for each oxidation state of the manganese. This shows that copper must be present in both Td and Oh sites, which is in accordance with the results found in the literature [13,14,18].

Many XPS studies on mixed metal oxides have shown the segregation or depletion of some elements at the surface [9,17,23,24]. Such behaviors come from surface relaxation and can generally be explained by energetic and steric (ionic radius) considerations. Kingery [25] claims that the dominant factor which determines the segregation is the size of the segregating cation (the larger the size, the stronger the enrichment at the surface). However, experimental results do not always fit this size effect and other parameters must then be considered as well. For example, Yang et al. [26] invoked the role of the synthesis atmosphere, and explained the surface segregation of Mn^{4+} cations in mixed Mn–Cu–Co oxides calcined in air by the fact that the Mn–O bonds are stronger than Cu–O and Co–O in the simple oxides MnO_2, CuO and Co_3O_4 [26]. According to these authors, the oxidative atmosphere attracts Mn at the surface more than Cu or Co, which induces a surface enrichment of Mn.

The surface atomic ratio Ni/Mn of nickel manganites was determined from XPS data using the sensitivity factors given by Wagner et al. [27]. This ratio was compared to that corresponding to the bulk composition and the results are reported in Fig. 6. This graph shows the surface enrichment of nickel for all the oxides: the higher the nominal nickel content of the oxide, the more segregated nickel at the surface. Sazonov et al. [28] have shown that the surface oxygen binding energies for NiO and MnO_2 were of a similar order. Therefore the interpretation of Yang et al. [26] cannot be invoked here. Actually, Ni^{2+} cations have a larger size than manganese cations and the size effect described by Kingery [25] may thus explain the surface segregation of nickel.

The surface chemical composition of nickel–copper manganites has also been investigated in a similar way. Table 6 shows that nickel still segregates at the surface. For a given nickel content ($x_{Ni} = 0.70$), the presence of copper in the oxides does not seem to influence the amount of segregated nickel cations. On the contrary, the surface atomic ratio Cu/(Mn + Ni) for $Ni_{0.70}Cu_yMn_{2.3-y}\square_{3\delta/4}O_{4+\delta}$ (Fig. 7) is lower than the corresponding bulk ratio. This difference between the two ratios increases with the nominal copper content of the

Table 6
Comparison of the surface (XPS) and bulk Ni/(Mn + Cu) atomic ratios for nickel–copper manganites with $x_{Ni} = 0.70$

y_{Cu} in $Ni_{0.70}Cu_yMn_{2.3-y}\square_{3\delta/4}O_{4+\delta}$	Ni/(Mn + Cu)XPS	Ni/(Mn + Cu) bulk
0	0.53	0.30
0.65	0.52	0.30
0.75	0.58	0.30
0.91	0.56	0.30

oxide. These results are opposite to those obtained by Veprek et al. [23] who showed the surface enrichment of copper at the surface of commercial Hopcalite $CuMn_2O_4$. However, the presence of nickel could explain the different behavior. Indeed, nickel and copper may compete for a surface exposition. Moreover, Yang et al. [26] have underlined the strong influence of the synthesis conditions of the samples, and particularly the atmosphere, on the resulting surface segregation. However, Anderson and Fierro [29] have observed a similar copper depletion for $LaZr_{1-x}Cu_xO_3$ perovskites. They attributed this phenomenon to the existence of highly-dispersed phases containing copper, like CuO. Until now, no experimental results have allowed us to show the existence of such highly-dispersed phases in our samples. However, this eventuality cannot be excluded and further surface analyses with other techniques will be necessary to investigate this point.

4. Conclusions

The surface of non-stoichiometric nickel and nickel–copper manganites has been investigated by XPS. The analysis of the Ni 2p core level only showed the presence of bivalent nickel. A chemical shift of ca. −1.5 eV in the Ni $2p_{3/2}$ region was observed between nickel and nickel–copper manganites. This was explained by the displacement of some Ni^{2+} cations from tetrahedral to octahedral sites of the spinel structure. The Cu $2p_{3/2}$ region of nickel–copper manganites was also investigated and the resulting XP spectra revealed the presence of both Cu^{+} and Cu^{2+} cations. The occurrence of metallic copper Cu° was ruled out by the determination of the modified Auger parameter. Moreover, the XPS data have shown the increase in proportion of bivalent copper compared to monovalent copper when the nominal copper content of the oxide increases. The analysis of the Mn $2p_{3/2}$ level of the oxides showed the simultaneous presence of the three oxidation states Mn^{2+}, Mn^{3+} and Mn^{4+} of the manganese in all the samples. The surface atomic ratios Ni/Mn and Ni/(Cu+Mn) were determined and compared to the corresponding bulk ratios. In all cases Ni^{2+} surface enrichment was observed. On the contrary, the surface ratio Cu/(Mn+Ni) was shown to be lower than that of the bulk. This behavior could be explained either by the presence of Ni leading to a penetration of Cu into the bulk or by the existence of Cu-containing highly-dispersed phases, such as CuO, on the surface of the samples.

References

[1] Hashemi T, Brinkman AW. J Mater Res 1992;7–5:1278.
[2] Hashemi T. Br Ceram Trans J 1991;90:171.
[3] Brabers VAM, Van Setten FM, Knapen PSA. J Sol Stat Chem 1983;49:93.
[4] Drouet C, Alphonse P, Rousset A, to be published.
[5] Drouet C, Alphonse P, Rousset A. Solid State Ionics 1999;123:25.
[6] Wagner CD, Riggs WM, Davis LE, Moulder JF, Muilenberg GE, Handbook of X-ray photoelectron spectroscopy, Perkin-Elmer, Minnesota, USA 1979.
[7] Rojas ML, Fierro JLG. J Sol Stat Chem 1990;89:299.
[8] Ertl G, Hierl R, Knözinger H, Thiele N, Urbach HP. Appl Surf Sci 1980;5:49.
[9] Allen GC, Harris SJ, Jutson JA, Dyke JM. Appl Surf Sci 1989;37:111.
[10] Lenglet M, D'Huysser A, Arsène J, Bonnelle JP, Jorgensen CK. J Phys C: Solid State Phys 1986;19:L363.
[11] Navrotsky A, Kleppa OJ. J Inorg Nucl Chem 1967;29:2701.
[12] Lenglet M, D'Huysser A, Bonnelle JP, Dürr J, Jorgensen CK. Chem Phys Lett 1987;136–5:478.
[13] Töpfer J, Feltz A, Dordor P, Doumerc JP. Mat Res Bull 1994;29–3:225.
[14] Lenglet M, D'Huysser A, Kasperek J, Bonnelle JP, Dürr J. Mat Res Bull 1985;20:745.
[15] D'Huysser A, Le Calonnec D, Lenglet M, Bonnelle JP, Jorgensen CK. Mat Res Bull 1984;19:1157.
[16] Töpfer J, Feltz A. Solid State Ionics 1993;59:249.
[17] Brabers VAM. Mat Res Bull 1983;18:861.
[18] Elbadraoui E, Baudour JL, Bouree F, Gillot B, Fritsch S, Rousset A. Solid State Ionics 1997;93:219.
[19] Brabers VAM, Van Setten F. J Phys D: Appl Phys 1983;16:L169.
[20] Sheffer GR, King TS. J Catal 1989;115:376.
[21] Töpfer J, Feltz A, Gräf D, Hackl B, Raupach L, Weissbrodt P. Phys Stat Sol (a) 1992;134:405.
[22] Martinez Sarrion ML, Morales M. J Am Ceram Soc 1995;78:915.
[23] Veprek S, Cocke DL, Kehl S, Oswald HR. J Catal 1986;100:250.
[24] Laine J, Brito J, Severino F, Castro G, Tacconi P, Yunes S, Cruz J. Catal Lett 1990;5:45.
[25] Kingery WD. Pure Appl Chem 1984;56:1703.
[26] Yang BL, Chan SF, Chang WS, Chen YZ. J Catal 1991;130:52.
[27] Wagner CD, Davis LE, Zeller MV, Taylor JA, Raymond RH, Gale LH. Surf Interface Anal 1981;3–5:211.
[28] Sazonov BA, Popovskii VV, Boreskov GK. Kin i Katal 1968;9–2:312.
[29] Anderson JA, Fierro JLG. J Sol Stat Chem 1994;108:305.